

Local Impurity Deposition in a Magnetic Island by Means of a Tracer-Encapsulated Solid Pellet in the LHD

TAMURA Naoki¹⁾, SUDO Shigeru^{1,2)}, KHLOPENKOV Konstantin V.²⁾,
KOSTRIOUKOV Artem Yu.²⁾, PETERSON Byron J.^{1,2)}, INAGAKI Shigeru²⁾,
NAGAYAMA Yoshio²⁾, KAWAHATA Kazuo^{1,2)}, MORISAKI Tomohiro^{1,2)}, IDA Katsumi²⁾,
OHYABU Nobuyoshi^{1,2)}, SUZUKI Hajime^{1,2)}, KOMORI Akio^{1,2)} and
LHD experimental groups²⁾

¹⁾Dept. of Fusion Science, Grad. Univ. Advanced Studies, Toki 509-5292, Japan

²⁾National Institute for Fusion Science, Toki 509-5292, Japan

(Received 29 July 2002 / Accepted 12 August 2002)

Local impurity deposition in the $n/m = 1/1$ magnetic island, which is expanded by the external perturbation coils, has been obtained by means of the tracer-encapsulated solid pellet in the Large Helical Device. The differences of the local deposition of the tracer between inside the magnetic island and outside that were clearly observed by both the absolute extreme ultra violet silicon photodiode arrays and the ECE radiometer.

Keywords: tracer-encapsulated solid pellet, magnetic island, impurity transport

The properties of heat and particle transport inside a magnetic island are important issues to be clarified, since the importance of magnetic islands for the plasma confinement has been emphasized recently [1]. In JET, when particles are fueled on the $q = 1$ surface by the frozen D_2 pellet injection, the oscillation in soft x-ray signals, called a “snake” has been observed [2]. This experimental result suggests that the particle diffusivity is low at the boundary of and/or inside the magnetic island.

A tracer-encapsulated solid pellet (TESPEL) has been developed for the advanced impurity particle transport study [3,4]. TESPEL consists of polystyrene as an outer shell and tracer particles as an inner core. Thus, TESPEL can produce a 3-dimensionally isolated particle source as a tracer. The Large Helical Device (LHD) has $n/m = 1/1$ external perturbation coils, which can control the size of the $n/m = 1/1$ magnetic island by changing the perturbation coil current, $I_{\text{ext-pc}}$. Figure 1 shows the successful example of the local impurity deposition in the $n/m = 1/1$ magnetic island by means of the TESPEL. In this case, $I_{\text{ext-pc}}$ is $-1,200$ A in order to expand the width of the magnetic island along the TESPEL

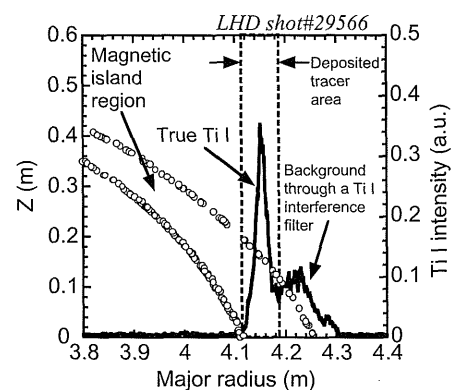


Fig. 1 Radial profiles of the light emission from the ablating TESPEL (solid line) and Cross-section of the magnetic island on the plane including the TESPEL injection axis (open circles).

injection axis (~ 14 cm). The TESPEL parameters are as follows: the outer diameter is $420 \mu\text{m}$, the velocity is 324 m/sec and the tracer consists of 3 titanium balls (diameter: $80 \mu\text{m}$, $60 \mu\text{m}$, $100 \mu\text{m}$, respectively). The line-averaged electron density and the central electron temperature just before the TESPEL injection are $1.0 \times$

author's e-mail: ntamura@LHD.nifs.ac.jp

10^{19} m^{-3} and $\sim 2.6 \text{ keV}$, respectively. The solid line in Fig. 1 indicates the radial profiles of the light emission from the ablating TESPEL and the open circles in Fig. 1 show the boundary of the magnetic island ($I_{\text{ext-pc}} = -1,200 \text{ A}$). This boundary of the magnetic island is calculated under vacuum conditions. Since the ratio of the plasma pressure to the magnetic pressure in this discharge is estimated as only 0.09% by the magnetic diagnostics, the calculated boundary for vacuum still can be applicable for this case. The light emission from the ablating tracer is indicated as the sharp peak of the solid line, which is framed by dashed lines. The other part of the line is due to light emissions from carbon, included in the polystyrene as the outer shell of the TESPEL, through an interference filter for Ti I ($\lambda_{\text{center}} = 400.3 \text{ nm}$, $d\lambda = 2.0 \text{ nm}$), as confirmed by the TESPEL injection without the tracer. Thus, the penetration of the tracer has stopped approximately at the inner boundary of the magnetic island. The range of the TESPEL penetration can be evaluated also with ECE signals. When the TESPEL does not penetrate over the inner boundary of the magnetic island, the maximum electron temperature drop in each channel caused by the TESPEL ablatant should appear after the TESPEL ablation at the region between the plasma center and the inner boundary of the

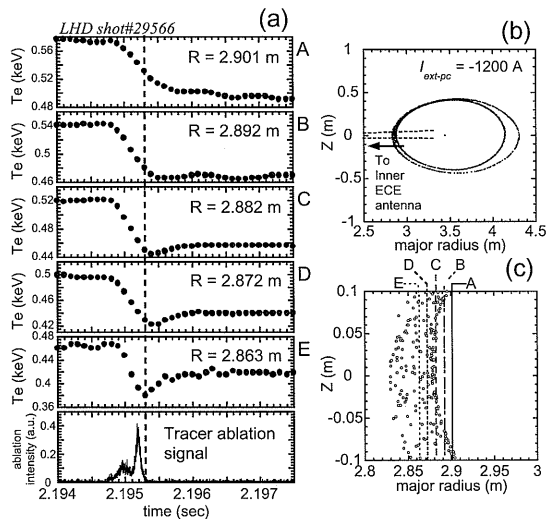


Fig. 2 In case of the local deposition of the tracer inside the magnetic island, (a) time evolutions of the electron temperature measured by the ECE radiometer and the tracer ablation signal, (b) observed area by the inner ECE antenna with the magnetic island, (c) the magnified figure of (b) at the vicinity of the magnetic island. The vertical dashed line in Fig. 2 (a) indicates the end time of the TESPEL ablation.

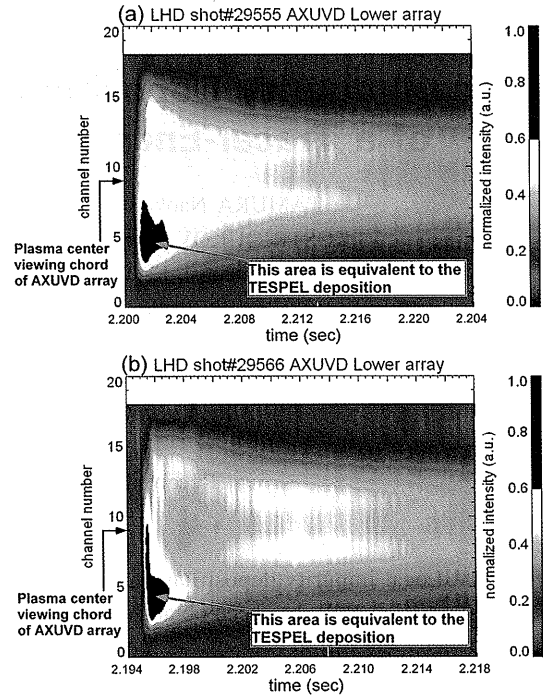


Fig. 3 Contour plots of the AXUVD signal increment due to the TESPEL injection in the case of (a) the local deposition of the tracer outside the magnetic island and (b) inside the magnetic island. Almost all the channels of the AXUVD array have a sightline of the magnetic island. The signal level is normalized to the peak value.

magnetic island. In the case of the successful example above, the maximum electron temperature drop at that region, such as $R = 2.901 \text{ m}$, appeared indeed after the TESPEL ablation, as compared with the case of $R = 2.892 \text{ m}$. The temporal evolution of the electron temperature at $R = 2.892 \text{ m}$ shows the ambiguous behavior in the vicinity of the inner boundary of the magnetic island. These experimental results also show that the tracer impurity has been deposited within the magnetic island.

As a reference, the TESPEL was injected toward the x point of the magnetic island ($I_{\text{ext-pc}}$ was set at $+800 \text{ A}$) so that the TESPEL may not be deposited in the magnetic island. In this case, as seen in Fig. 3 (a), the signal intensity of the absolute extreme ultra violet silicon photodiode (AXUVD), I_{AXUVD} was increased sharply with the TESPEL injection, especially in the channels viewing the location equivalent to the TESPEL deposition (ch. 4–6). (Note: the AXUVD can detect the light emissions in the energy range of 7 eV to 6,000 eV.) After the peak of the I_{AXUVD} increment, the I_{AXUVD} for all the channels decreases continuously. On the other

hand, as seen in Fig. 3 (b), in the case of the local deposition of the tracer inside the magnetic island ($I_{\text{ext-pc}} = -1,200$ A), just after the peak of the I_{AXUVD} increment ($t \sim 2.198$ sec), the profile of the I_{AXUVD} is expected as very hollow, even from the behavior of the line-integrated I_{AXUVD} . Subsequently the highly hollow profile for I_{AXUVD} evolves into a more peaked one approximately 6 msec after the TESPEL injection. In the end, the I_{AXUVD} decreased with a certain delay time, compared with the case as shown in Fig. 3 (a). This characteristic behavior might be explained as follows: Firstly, the tracer deposited locally inside the magnetic island has diffused inside the magnetic island. This diffusion within the magnetic island, which is located asymmetrically at the periphery of the plasma as seen in Fig. 2 (b), made the highly hollow profile for I_{AXUVD} as seen at $t \sim 2.198$ sec in Fig. 3 (b). Secondly the tracer has diffused outside the magnetic island. This caused the

changing of the profile shapes from highly hollow to more peaked.

In addition, in case that the TESPEL is almost not deposited inside the magnetic island, the propagation of the cold pulse produced by the TESPEL from the core into the expanded magnetic island has been observed clearly by the ECE radiometer. These experimental results indicate that the high localization of the TESPEL deposition will be useful for the heat and particle transport study of the magnetic island.

- [1] Y. Kamada *et al.*, Plasma Phys. Controll. Fusion **42**, A65 (2000).
- [2] R.D. Gill *et al.*, Nucl. Fusion **32**, 723 (1992).
- [3] S. Sudo., J. Plasma. Fusion Res. **69**, 1349 (1993).
- [4] S. Sudo., *et al.*, Plasma Phys. Controll. Fusion **44**, 129 (2002).